Influence of Alloying Elements and Effect of Stress on Anisotropic Hydrogen Diffusion in Zr-Based Alloys Predicted by Accelerated Kinetic Monte Carlo Simulations

Jianguo Yu, Chao Jiang and Yongfeng Zhang

Abstract The presence of hydrogen (H) can detrimentally affect the mechanical properties of many metals and alloys. To mitigate these detrimental effects requires fundamental understanding of the thermodynamics and kinetics governing H pickup and hydride formation. In this work, we focus on H diffusion in Zr-based alloys by studying the effects of alloying elements and stress, factors that have been shown to strongly affect H pickup and hydride formation in nuclear fuel claddings. A recently developed accelerated kinetic Monte Carlo method is used for the study. It is found that for the alloys considered here, H diffusivity depends weakly on composition, with negligible effect at high temperatures in the range of 600–1200 K. Therefore, the small variation in H diffusivity caused by variations in compositions of these alloys is likely not a major cause of the very different H pickup rates. In contrast, stress strongly affects H diffusivity. This effect needs to be considered for studying hydride formation and delayed hydride cracking.

Keywords Hydrogen diffusion · Zirconium alloys · Accelerated kinetic monte carlo

J. Yu (✉) · C. Jiang · Y. Zhang
Fuels Modeling and Simulation, Idaho National Laboratory,
Idaho Falls, ID 83415, USA
e-mail: jianguo.yu@inl.gov

C. Jiang
e-mail: chao.jiang@inl.gov

Y. Zhang
e-mail: yongfeng.zhang@inl.gov

J.H. Jackson et al. (eds.), *Proceedings of the 18th International Conference on Environmental Degradation of Materials in Nuclear Power Systems – Water Reactors*, The Minerals, Metals & Materials Series, https://doi.org/10.1007/978-3-030-04639-2_122

Introduction

Zirconium (Zr) alloys are extensively used as fuel cladding tubes in nuclear reactors owing to their low capture cross section to thermal neutron, good mechanical properties, and good corrosion resistance in various environmental conditions [1–3]. Most of current claddings are made of two Zr-based alloys [Zircaloy-2 (Zr2) and Zircaloy-4 (Zr4)]. Zr4 is mainly used in pressurized water reactors (PWRs) and Zr2 in boiling water reactors (BWRs). Significant effort has led to the development of modern Zr-based alloys with improved corrosion resistance and mechanical properties to meet the demands of higher fuel duty. For example, ZIRLO® and M5™ are more resistant to corrosion and hydrogen (H) pickup compared to Zr2 and Zr4, and they are used to replace Zr4 in PWRs. In addition, some other modern Zr-based alloys such as J-alloys and AXIOM™ have also been shown to not have enhanced corrosion at high burnups [1].

An interesting feature of these Zr-based claddings is that the addition or variation of a very small amount of alloying elements (typically less than 0.5% in concentration or weight) may be sufficient to dramatically change the corrosion behavior as well as H pickup fraction [1, 2] under operating conditions. For instance, with higher Fe content substituted for Ni, Zr4 (Zr-1.5Sn-0.2Fe-0.1Cr in wt%) was developed with significantly lower H pickup fraction compared to that exhibited by Zr-2 (with an approximate composition of Zr-1.5Sn-0.14Fe-0.10Cr-0.06Ni in wt%). For H to accumulate in the metal matrix of claddings, it needs to be produced during oxidation, and then transport over the oxide layer and eventually in the metal matrix. Therefore, the very different H pickup rates in various Zr-based alloys could be caused by (1) different oxidation kinetics and thus H production rates, (2) different transport speeds over the oxide layers [1] which have generally been regarded as an effective barrier to the absorption of hydrogen [3] and (3) different diffusion speeds in the metal matrix. However, it is not clear how the alloying elements will affect H diffusion, which is one of focuses in this study.

Another factor that may strongly affect H diffusion is stress. For instance, during hydride formation, stress may be induced by the mismatch between hydrides and the Zr matrix [3]. Upon cyclic thermal and mechanical loadings, hydrides can dissolve and reorient; this process involves H diffusion with the presence of stress. Meanwhile, stress may also be concentrated at crack tips during delayed-hydride-cracking (DHC). Zr-based alloy cladding tubes used in the nuclear industry are highly susceptible to DHC, which occurs when dissolved H atoms diffuse along the stress gradient towards the tensile stress concentration region at the crack tip, followed by reformation of hydrides at the crack tip and subsequent fracture [3, 4]. DHC may take place at stress levels much lower than the yielding stress and has remained a concern for cladding integrity during used fuel storage. A more comprehensive understanding on hydride reorientation and DHC requires a fundamental understanding of the stress state effect on the H diffusion.

In the past, a plethora of investigations on understanding of H diffusion in α-Zr and Zr alloys has been reported in the literature. However, most investigations

relied on experimental measurements [5–9]. It has been commonly accepted that H diffuses in Zr alloys via the same mechanism as in α-Zr, with additional trapping caused by alloying elements and impurities. Due to the hexagonal symmetry of α-Zr, the diffusivity of H along <c> usually differs from that along <a> (in a plane parallel to <a> and normal to <c>), with the former suggested to be higher than the latter with D_c/D_a >1, but not exceeding 2, at temperatures above 600 K by Kearns et al. [8]. In addition to these experiments, atomic scale studies such as density functional theory (DFT) calculations have also been applied to H diffusion in α-Zr [10–12].

H diffusion in α-Zr involves multiple hopping paths coupled with each other for long-range diffusion. The hopping rates obtained from DFT calculations need to be incorporated into either analytical theories or other modeling methods such as kinetic Monte Carlo (KMC) to predict diffusivity. One challenge to apply KMC to H diffusion in hcp metals is that the potential energy surface contains an energy basin formed by neighboring tetrahedral sites, which strongly limits the efficiency of KMC at low temperatures due to basin trapping. Since accurate H diffusivity is highly desired at low temperatures [4] to predict the kinetics of DHC, which is active in the temperature range of about 150 to 300 °C, acceleration of KMC is needed. Although guidance for general acceleration approaches already exists in the literature [13], analytical solutions that directly apply to interstitial diffusion in hcp crystals are yet to be derived. Recently an accelerated KMC method was developed for H diffusion in hcp metals by co-authors of this study [14]. Parameterized by DFT calculations, the accelerated KMC method is capable of efficiently calculating H diffusivity in a variety of Zr alloys, without altering the kinetics of long-range diffusion. Using this accelerated KMC method, this article is aimed at modeling H diffusion in Zr-based alloys under the influence of both alloying elements and stress.

Methods

DFT Calculations

To obtain the migration barriers for H diffusion as well as the binding energies between alloying elements (Sn, Fe, Cr, Ni, Nb) and H, we performed ab initio calculations using the all-electron projector augmented wave method within the generalized gradient approximation of Perdew, Burke, and Ernzerhof (PBE-GGA) [15], as implemented in VASP [16]. 96-atom supercells, which can be constructed from a 4 × 4 × 3 extension of the 2-atom hcp Zr unit cell, are used. Spin-polarized calculations are performed for Fe, Cr and Ni. A plane-wave cut-off energy of 500 eV and a 5 × 5 × 5 Monkhorst–Pack *k*-point mesh are used to ensure high numerical accuracy for total energy calculations. All internal atomic positions are fully optimized using a conjugate gradient method until forces are less than

0.01 eV/Å. Further relaxations of supercell volumes have been found to have negligible effect on the final results. To study the stress effect on H diffusion, the 96-atom hcp Zr supercell is hydrostatically strained by −2, −1, 0, +1 and +2%, respectively. The corresponding hydrostatic stress is 6.2, 2.9, 0, −2.7 and −5.1 GPa, respectively. Such stress levels can be reached at crack tips and at hydride/matrix interfaces. More computational details can be found in Ref. [14].

Accelerated Lattice Kinetic Monte Carlo

The accelerated KMC method recently developed by co-authors [14] is used in this article. For acceleration, the KMC events in basins are replaced using the solutions detailed in Ref. [14]. The calculations are performed from 300 to 1200 K, one data point every 100 K, covering the temperature range used in previous experiments. To minimize stochastic scattering, at each temperature 100,000 KMC simulations are carried out, each lasting until 100,000 basin exits are detected for sufficient statistics. The averaged mean-square-displacements (MSD) display the expected linear relationship with time, with the slope proportional to diffusivity.

Results and Discussion

Results from DFT Calculations

The calculated binding energies between H and alloying elements are listed in Table 1. For Sn, Fe, Cr, and Ni, the results have been previously reported in Ref. [14]. As mentioned in Ref. [14], there exist three different interactions between H and an impurity within the first nearest neighbor (1NN) distance. A binding energy of E_b^O represents octahedral (O) H trapped by one impurity site within 1NN distance, $E_b^{T_c}$ is for tetrahedral (T) H interstitials trapped by one impurity site within 1NN distance along <c> and $E_b^{T_a}$ denotes tetrahedral H interstitials trapped by one impurity site within 1NN distance in the basal plane. As shown in Table 1, Fe, Cr and Ni are attractive to H while Sn is repulsive to H. However, the binding energies between H and Nb are unusual. Specifically, the interaction is weakly repulsive when H occupies the tetrahedral sites, but attractive when H is at the octahedral site. As will be shown later by KMC simulations, such unusual feature of the binding energies between H and Nb can lead to lower anisotropic ratio of H diffusivity in Zr alloy system containing Nb element.

The activation barriers versus strain predicted by DFT calculations are given in Table 2 and plotted in Fig. 1a. Under compressive stress, the activation barriers for all four hopping paths increase. Under tensile stress, the activation barriers for all four hopping paths decrease. It is also shown that, although the activation barriers

Table 1 Binding energies [eV] between H and alloying elements from DFT calculations. Positive (negative) binding energy means attractive (repulsive) interaction. Results for Sn, Fe, Cr, and Ni are from Ref. [14]

Element	$E_b^{T_c}$	$E_b^{T_a}$	E_b^{O}
Sn	Not stable [14]	Not stable [14]	−0.037 [14]
Fe	0.094 [14]	0.069 [14]	0.106 [14]
Cr	0.089 [14]	0.065 [14]	0.085 [14]
Ni	0.212 [14]	0.153 [14]	0.165 [14]
Nb	−0.0024	−0.0007	0.042

Table 2 H migration barriers [eV] versus applied hydrostatic strains and the corresponding stresses [GPa] for 1NN jumps from DFT calculations

Pressure [GPa]	T-T	T-O	O-T	O-O	Strain %
6.247	0.14592	0.42383	0.45171	0.52806	−2.0
2.942	0.13576	0.41658	0.3984	0.46177	−1.0
0	0.12952	0.40612	0.34574	0.39849	0.0
−2.71	0.1251	0.39299	0.29653	0.33965	1.0
−5.134	0.12328	0.37747	0.24796	0.28139	2.0

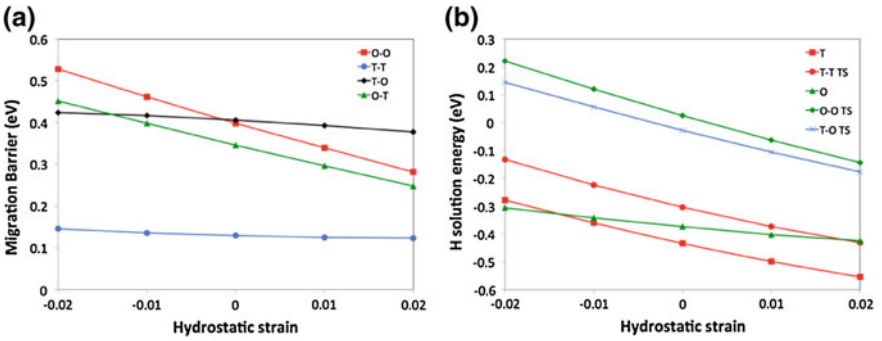

Fig. 1 DFT calculated H migration barrier (**a**) and H solution energy (**b**) in hcp Zr as a function of hydrostatic strain

for all four hopping paths depend nearly linearly on the applied stress, the activation barriers for the O-T and O-O jumps are much more significantly modified by the applied stress compared with T-T and T-O jumps. This can be understood since the O site is significantly larger than the T site and the transition states (TSs) volumetrically. Therefore, the solution energy of a H atom at the O site will exhibit much weaker pressure dependence compared with a H at the TS for either O-T or O-O jump (see Fig. 1b). Conversely, as shown in Fig. 1b, H atom at a T site exhibits very similar pressure-dependent behavior as the H atom at the TS for either T-T or T-O jump. The migration barrier, which is the energy difference between TS and T, therefore shows weak pressure dependence for T-T and T-O jumps. It is also

interesting to note that, under compressive stress, the O site can become more favorable than T site for H occupation. This is due to the fact that H energy at T site increases much faster with pressure than at O site.

Hydrogen Diffusion in Zr Alloys

KMC simulations are carried out to study the effect of alloy elements on H transport in Zr alloys. The corresponding approximate concentrations of the alloying elements of Zr alloys used in the KMC simulations are listed in Table 3. J3 (Zr-2.5Nb in wt%) alloy in the J-Alloys family (used extensively in pressure tubes in Canada Deuterium Uranium (CANDU) nuclear reactors [4]) is considered in this study. The results for the three-dimensional H diffusivity and the anisotropic diffusivity ratio in a variety of Zr alloys calculated are plotted in Fig. 2. As shown in Fig. 2 (a), at high temperatures in the range of 600–1200 K, the variation of H diffusivity in the Zr alloys studied here is very small. This indicates that the addition of alloying elements slightly reduces H diffusivity, with negligible effect at high temperatures. This observation is also in line with previous experiments, which found similar H diffusivity in α-Zr, Zr2, and Zr4 [8]. Using $D = D_0 \exp(-E_m/K_B T)$ with D_0 being the prefactor and E_m the effective migration barrier, fitted parameters for D_0 and E_m using the KMC results are listed in Table 4. The fitted results agree nicely with previously KMC values of 1.08×10^{-6} m^2/s and 0.46 eV shown in Fig. 2 (a) [14] and the averaged values of 7.0×10^{-7} m^2/s and 0.46 eV for α-Zr and Zircaloy from experiments [8]. At room temperature, the diffusivity of H in Zr2 is significantly lower than those of other alloys, presumably due to its higher concentration

Table 3 Approximate concentrations c_i (atomic fraction) of Sn, Fe, Cr, Ni and Nb in a variety of Zr alloys

Alloy	Sn	Fe	Cr	Ni	Nb
Zircaloy-2	0.011526	0.002287	0.001754	0.000932	0
Zircaloy-4	0.009990	0.003267	0.001754	0	0
ZIRLO®	0.007684	0.001633	0	0	0.009819
Optimized ZIRLO™	0.005149	0.001633	0	0	0.009819
J-Alloys					
J1	0	0	0	0	0.017674
J2	0	0	0.001754	0	0.015710
J3	0	0	0	0	0.024547
AXIOM™ alloys					
X2	0	0.000980	0	0	0.009819
X5	0.002305	0.005717	0.004386	0.000777	0.006873
X5A	0.003458	0.005717	0.004386	0	0.002946

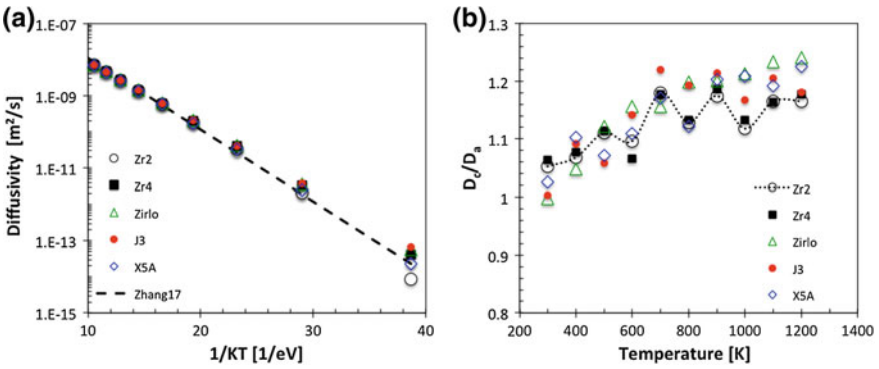

Fig. 2 **a** H diffusivity in Zr alloys of Zr2, Zr4, Zirlo, J3 and X5A as a function of inverse temperature, 1/KT; **b** D_c/D_a ratio from 300 to 1200 K

Table 4 Fitting of the KMC results using $D = D_0 \exp(-E_m/K_B T)$

	D_0 [m^2/s]	E_m [eV]
Zhang17 [14]	1.08×10^{-6}	0.46
Zr2	1.08×10^{-6}	0.457
Zr4, ZIRLO, J3	7.0×10^{-7}	0.425
X5A	9.0×10^{-7}	0.448

of Ni that strongly traps H atoms. Intriguingly, the lower H diffusivity in Zr2 than in Zr4 is in contrast with the lower H pickup in the latter. Therefore, the present results suggest that H diffusion in the metal matrix may not be the reason for the very different H pickup in various cladding alloys.

As shown in Fig. 2b, the diffusivity of H is anisotropic, which is in line with previous experiments [8] and KMC results [14]. In particular, the ratio of $D_c/D_a > 1$ is observed at temperatures above 400 K. The addition of alloying elements is found to have little effect on the anisotropy. For all alloys studied here, the ratio of D_c/D_a is about 1 at room temperature and increases with increasing temperature. A plateau at about 1.2 is reached at high temperatures, similar to the behavior of H in pure Zr [4]. Some stochastic effect is also noticed in the KMC results shown in Fig. 2b.

Stress Effect on Hydrogen Diffusion

To explore the effect of stress, the diffusivity of H in a variety of Zr alloys with 5 different applied hydrostatic stresses (6.2, 2.9, 0, −2.7 and −5.1 GPa, respectively) have been studied. The KMC simulation results for the stress effect on H diffusivity for Zr2, Zr4, Zirlo, J3 and X5A alloys are plotted in Figs. 3, 4, 5, 6 and 7, respectively. As expected, the H diffusivity is reduced under compressive stress and

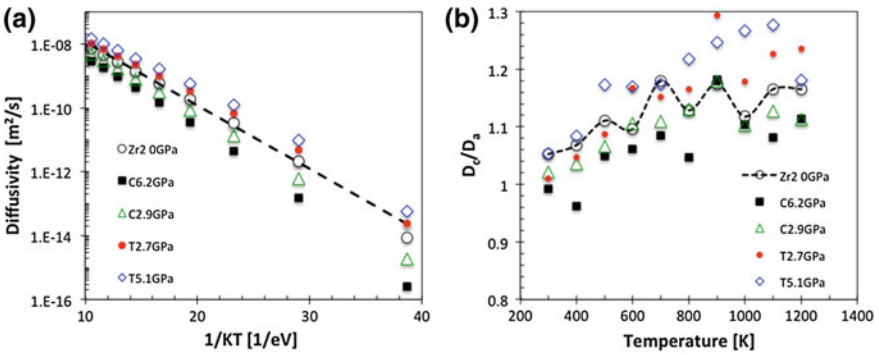

Fig. 3 Effect of stress on (**a**) H diffusivity in Zr2 alloy as a function of inverse temperature, 1/KT; (**b**) D_c/D_a ratio from 300 to 1200 K

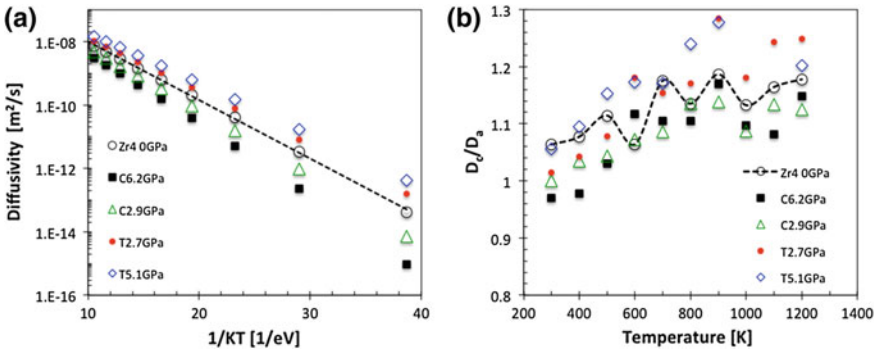

Fig. 4 Effect of stress on (**a**) H diffusivity in Zr4 as a function of inverse temperature, 1/KT; (**b**) D_c/D_a ratio from 300 to 1200 K

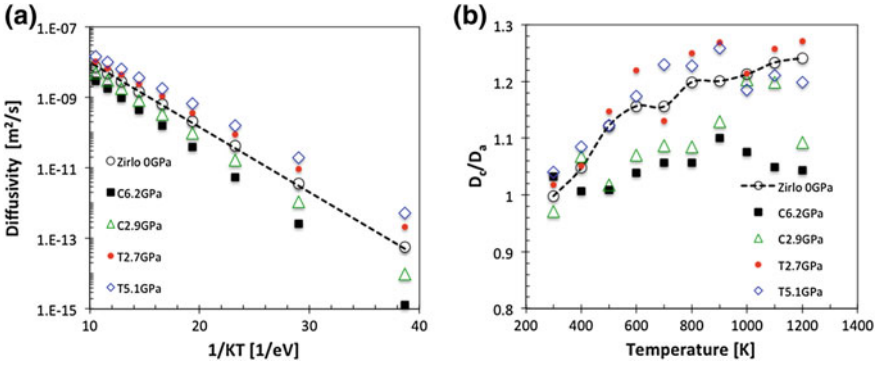

Fig. 5 Effect of stress on (**a**) H diffusivity in Zirlo as a function of inverse temperature 1/KT; (**b**) D_c/D_a ratio from 300 to 1200 K

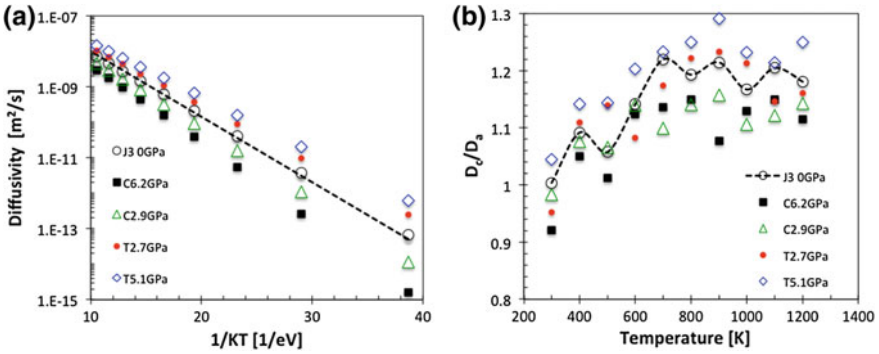

Fig. 6 Effect of stress on (**a**) H diffusivity in J3 as a function of inverse temperature, 1/KT; (**b**) D_c/D_a ratio from 300 to 1200 K

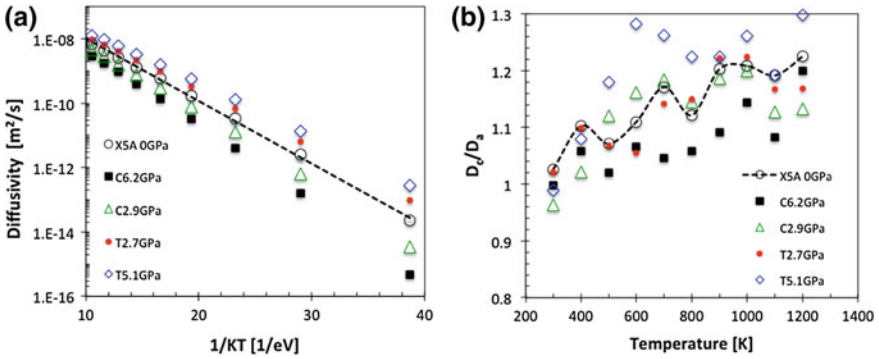

Fig. 7 Effect of stress on (**a**) H diffusivity in X5A as a function of inverse temperature, 1/KT; (**b**) D_c/D_a ratio from 300 to 1200 K

increased under tensile stress. Furthermore, the ratio D_c/D_a depends on both temperature and pressure. In all five Zr alloys considered, a general trend can be seen that both temperature and tensile stress will increase the D_c/D_a ratio and thus promote the anisotropy. At room temperature and under compressive stress, the ratio D_c/D_a can also become less than 1.

Elastic Dipole Tensor

It is also desired to have analytical descriptions for the dependence of migration barriers on elastic strain. Based on the theory of linear elasticity, the interaction energy between an external strain field ε_{ij} and a point defect can be calculated from its elastic dipole tensor P_{ij} as [17]:

Table 5 Elastic dipole tensors P_{ij} for H at various interstitial sites and transition states in hcp Zr

Site	P_{11} (eV)	P_{22} (eV)	P_{33} (eV)
T	1.999	1.999	3.265
O	0.779	0.779	1.313
T-T TS	3.404	3.404	1.174
O-O TS	3.105	3.105	3.801

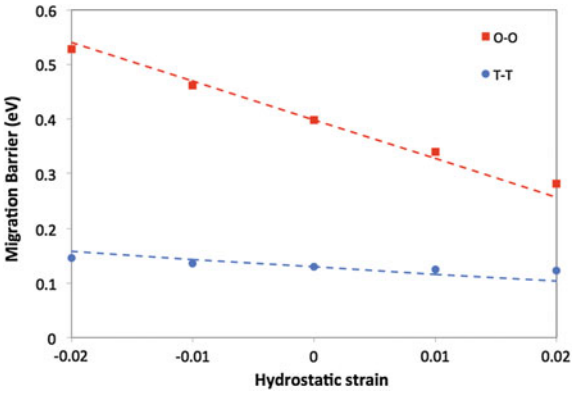

Fig. 8 Migration barriers for O-O and T-T paths in hcp Zr as a function of applied hydrostatic strain. Solid symbols are from the present DFT calculations. Solid lines represent results from elastic calculations

$$\Delta E = -\sum_{ij} P_{ij}\varepsilon_{ij} \tag{1}$$

In this study, we have calculated the elastic dipole tensors for H at O, T, and TS positions in hcp Zr using DFT. The results are reported in Table 5 and plotted in Fig. 8. The computational details can be found in Ref. [17]. Due to its low symmetry, the elastic dipole tensor of the TS for the T-O jump is not calculated here. As shown in Fig. 8, results from elastic theory calculations agree quantitatively with direct DFT calculations. Such a good agreement suggests that Eq. (1) can be used to accurately describe H diffusion behavior under an elastic stress field (e.g. around a crack tip) in hcp Zr. It also indicats that the effect of stress on H diffusion is most likely dominated by the elastic interaction.

Conclusion

In this work, an accelerated KMC method is used to reveal the influence of alloying elements and the effect of applied stress on H diffusivity in hcp Zr alloys. It is found that at very low temperature around ambient, H diffusivity might depend on the addition of alloying elements. However, at high temperatures in the range of 600-1200 K, the discrepancy of H diffusivity in the Zr alloys studied here is very

small. This indicates that the addition of alloying elements has negligible effect at high temperatures on H diffusivity, and this is likely not the reason for the very different H pickup in various cladding alloys. Applied stress is found to have a stronger effect on H diffusion than alloying elements. H diffusivity decreases under compressive and increases under tensile stress. Such change in H diffusion needs to be considered at stress fields induced by crack tips or hydrides.

Acknowledgements We gratefully acknowledge the support of the Department of Energy (DOE) Nuclear Energy Advanced Modeling and Simulation (NEAMS) program. This manuscript has been authored by Battelle Energy Alliance, LLC under Contract No. DE-AC07-05ID14517 with the U.S. Department of Energy. The United States Government retains and the publisher, by accepting the article for publication, acknowledges that the United States Government retains a nonexclusive, paid-up, irrevocable, world-wide license to publish or reproduce the published form of this manuscript, or allow others to do so, for United States Government purposes.

References

1. A.T. Motta, A. Couet, R.J. Comstock, Corrosion of zirconium alloys used for nuclear fuel cladding. Annu. Rev. Mater. Res. **45**, 311–343 (2015)
2. S.J. Zinkle, K.A. Terrani, L.L. Snead, Motivation for utilizing new high-performance advanced materials in nuclear energy systems. Curr. Opin. Solid State Mater. Sci. **20**, 401–410 (2016)
3. T. Allen, R. Konings, A. Motta, Corrosion of zirconium alloys. Compreh. Nuclear Mater. **5**, 49–68 (2012)
4. K.S. Chan, An assessment of delayed hydride cracking in zirconium alloy cladding tubes under stress transients. Int. Mater. Rev. **58**, 349–373 (2013)
5. A. Sawatzky, The diffusion and solubility of hydrogen in the alpha-phase of zircaloy-2. J. Nucl. Mater. **2**, 62–68 (1960)
6. C.M. Schwartz, M.W. Mallett, Observations on the behavior of hydrogen in zirconium. Trans. Am. Soc. Metals **46**, 640–654 (1954)
7. J.J. Kearns, Terminal solubility and partitioning of hydrogen in alpha phase of zirconium zircaloy-2 and zircaloy-4. J. Nucl. Mater. **22**, 292–303 (1967)
8. J.J. Kearns, Diffusion coefficient of hydrogen in α-Zr, Zircaloy2 and Zircaloy4. J. Nucl. Mater. **43**, 330–338 (1972)
9. C.S. Zhang, B. Li, P.R. Norton, The study of hydrogen segregation on Zr (0001) and Zr(10(1) over-bar0) surfaces by static secondary ion mass spectroscopy, work function, Auger electron spectroscopy and nuclear reaction analysis. J. Alloy. Compd. **231**, 354–363 (1995)
10. D.S. Sholl, Using density functional theory to study hydrogen diffusion in metals: a brief overview. J. Alloy. Compd. **446**, 462–468 (2007)
11. M. Christensen, W. Wolf, C. Freeman, E. Wimmer, R.B. Adamson, L. Hallstadius, P.E. Cantonwine, E.V. Mader, H in alpha-Zr and in zirconium hydrides: solubility, effect on dimensional changes, and the role of defects. J. Phys.-Conden. Matter **27**, 025402 (2015)
12. C. Domain, R. Besson, A. Legris, Atomic-scale Ab-initio study of the Zr-H system: i bulk properties. Acta. Materialia. **50**, 3513–3526 (2002)
13. B. Puchala, M.L. Falk, K. Garikipati, An energy basin finding algorithm for kinetic Monte Carlo acceleration. J. Chem. Phys. **132**, 134104 (2010)
14. Y.F. Zhang, C. Jiang, X.M. Bai, Anisotropic hydrogen diffusion in alpha-Zr and Zircaloy predicted by accelerated kinetic Monte Carlo simulations. Sci. Rep. **7**, 41033 (2017)

15. J.P. Perdew, K. Burke, M. Ernzerhof, Generalized gradient approximation made simple. Phys. Rev. Lett. **77**, 3865–3868 (1996)
16. G. Kresse, J. Furthmuller, Efficient iterative schemes for ab initio total-energy calculations using a plane-wave basis set. Phys. Rev. B **54**, 11169–11186 (1996)
17. R. Agarwal, D.R. Trinkle, Light-element diffusion in Mg using first-principles calculations: Anisotropy and elastodiffusion. Phys. Rev. B **94**, 054106 (2016)